

MORPHOLOGY OF INTERMETALLIC (Co-Sn, Ni-Sn) NANOPARTICLES, ELECTROCHEMICALLY TESTED AS ELECTRODES IN Li-ION BATTERY

Valentina Milanova¹, Stela Atanasova², Georgy Avdeev², Ivania Markova¹

¹ University of Chemical Technology and Metallurgy
8 Kl. Ohridski, Sofia, Bulgaria

Received 14 July 2016

Accepted 12 December 2016

² Institut of Physical Chemistry
Bulgarian Academy of Sciences
1, Akad. G. Bonchev str., bl. 11, 1113 Sofia, Bulgaria
E-mail: vania@uctm.edu

ABSTRACT

Intermetallic Co-Sn and Ni-Sn nanoparticles were synthesized by a template technique with a support, through a borohydride reduction method in a mixture of aqueous solutions respectively of $\text{CoCl}_2 \cdot 6\text{H}_2\text{O}$, $\text{NiCl}_2 \cdot 6\text{H}_2\text{O}$ and $\text{SnCl}_2 \cdot 2\text{H}_2\text{O}$ at a pre-set ratio of Co:Sn, respectively Ni:Sn, at room temperature and atmospheric pressure. Fluorinated graphite (CF) was used as the template and sodium borohydride as the reducing agent. In order to form uniform and finely monodispersed nanocrystals, β -cyclodextrine (β -CDx) was employed as a capping agent and citric acid ($\text{C}_6\text{H}_8\text{O}_7$), as a stabilizing ligand. The morphology, structure, elemental and phase compositions of the obtained carbon-based nanocomposite materials with Co-Sn and Ni-Sn nanoparticles, were investigated with scanning and transmission electron microscopy (SEM/TEM), energy dispersive analysis (EDS) and X-ray diffraction analysis (XRD). The nanocomposites were characterized before and after being electrochemically tested as electrodes in a Li-ion battery through a cycling voltammetry. After the electrochemical tests the samples remained homogeneous and compact, and no cracking was observed. This shows that during the processes of charge/discharge the tested samples keep their mechanical stability.

Keywords: intermetallic nanoparticles, borohydride reduction, template technique, support, graphite, β -cyclodextrine, morphology, SEM, EDS, XRD.

INTRODUCTION

Due to the fastly increasing development of electronic devices in recent years, the need of new, highly effective and ecologically friendly materials for electrodes in batteries and electrochemical energy storage systems becomes evident.

Graphite carbon is an active anode material, used in conventional Li-ion batteries. Its electrochemical behavior depends on its microstructure and morphology. Furthermore, graphites show relatively low theoretical gravimetric and volume capacities that cannot yet cover the demands and the new requirements of the market for highly energetic systems. Some problems are due to the continuous and safe work of the graphite anode. The electrochemical process is exothermal and

local superheatings occur. Another disadvantage of the graphite electrode is the possibility for dendrites to be formed during the process of lithiation, because of the low working potential. That enforces the demand for safer alternatives [4, 5, 7].

During the cycle of charge/discharge the volume of the graphite electrodes changes quickly. This causes the forming of cracks and destruction of the electrode. For this reason they are not used in the commercial manufacturing of batteries. This negative effect can be minimized by creating composite (bi- or multiphase) electrodes or by decreasing the size of the receiving material (the electrode). At the bi- or multiphase electrodes the active material (Sn) is usually surrounded by an inert (non reacting) phase (Cu, Co, Ni), which serves as a buffer, increasing the mechanical stability of the electrode.

Decreasing the size of the particles in the electrode is also an effective way to reduce the volume change, the mechanical stress and the material cracks, respectively.

That is why, recently the investigations are focused on preparing metal alloys and intermetallic compounds, e.g. nanosized intermetallic compounds for electrode materials, to replace the graphite electrode, currently used as anode in Li-ion batteries. Such compounds are based on Co, Ni, and Sn. They are used in both the scientific and the industrial spheres, because of their improved characteristics, as compared to those of pure metals [1-24]. There is a great interest for nanosized intermetallic compounds to be used as electrode materials and replace the graphite electrode in Li-ion batteries. These materials have higher volumetric capacity compared with graphite.

Various methods and techniques are used for preparing nanosized alloys with a different morphology, such as a high energy ball milling (mechanical alloying and sintering), melting together with spinning, electrostatic spray reductive precipitation, vapour deposition, electrospinning, electrochemical deposition, chemical methods, carbon-thermal reduction [4,7, 13 - 15, 18, 19, 22, 23].

Chemical reduction with sodium borohydride (NaBH_4) is a well known technology and is often applied for obtaining cathode materials for Li-ion batteries [26 - 28]. This method is based on the so-called „bottom-up” technique, opposite to the „top-down” technique, used with mechanical methods. Changing some parameters, such as concentration of the precursors, temperature, and use of different surfactants, can control the size of the obtained particles and their morphology. The chemical reduction of metal chlorides with NaBH_4 is a method that can be carried out in both water and organic solutions, while an effective control of the size of the obtained nanoparticles can be achieved. The borohydride reduction can sometimes be combined with an electrostatic spray pyrolysis of the precursors, known as the ESRP method [3]. By combining these two technologies fine monodisperse nanoparticles are obtained.

According to literature data nanoparticles with good dispersity and low aggregation can be prepared using cyclodextrines as a capping agent during the synthesis [10, 24]. Cyclodextrines are characterized with structure that consists of a hydrophobic hollow and a hydrophilic surface.

Their specific structure allows for the formation of complexes when interacting with hydrophobic molecules. Cyclodextrines are used in different scientific

fields, such as electroanalysis, biotechnologies and environmental studies, due to their specific physical and chemical characteristics. For example, the interaction of β -cyclodextrine with the binding agent epichlorohydrine results in polymers, which selectively form complexes. The functionalization of the carbon-containing composite nanomaterials with such polymers gives them unique properties.

The combination of the unique properties of carbon (graphite) with those of the intermetallic nanoparticles, determines the carbon C-based nanoparticles composites as perspective materials for new generation electrodes in the modern electrochemical energy storage systems. The potential of carbon-based nanocomposites with intermetallic nanoparticles and the obtained results concerning the synthesis of intermetallic nanoparticles with a carbon-containing matrix, determined the aims of this work. First, to synthesize Co-Sn and Ni-Sn nanoparticles through a borohydride reduction, using a template technique with a matrix of graphite and also graphite, in the presence of β -cyclodextrine, and thus to obtain in situ carbon-containing composite materials. Second, to investigate the morphology, structure, elemental and phase composition of the intermetallic nanoparticles and their carbon based composites, before and after running electrochemical tests to study their mechanical strength during the charge/discharge processes.

EXPERIMENTAL

Synthesis of intermetallic Co-Sn nanoparticles at a ratio Co:Sn = 35:65 and their carbon-containing nanocomposites

The intermetallic Co-Ni nanoparticles were synthesized through the borohydride reduction method with 0.5M NaBH_4 in a mixture of aqueous solutions of 0.2M $\text{CoCl}_2 \cdot 6\text{H}_2\text{O}$ and 0.2M $\text{SnCl}_2 \cdot 2\text{H}_2\text{O}$, at a ratio Co:Sn=35:65. To reach the ratio chosen according to the phase diagram of the binary Co-Sn system, we used 20 ml 0.2M $\text{CoCl}_2 \cdot 6\text{H}_2\text{O}$ and 36 ml 0.2M $\text{SnCl}_2 \cdot 2\text{H}_2\text{O}$. To fully complete the reduction process, the quantity of the reducing agent stabilized with NaOH was 55ml 0.5M NaBH_4 , i.e. approximately equal to the sum of the quantities of the precursor solutions. Citric acid ($\text{C}_6\text{H}_8\text{O}_7$) was used as a stabilizing ligand, in a quantity of 0.44 g.

The synthesis was carried out in a double-wall cell to keep a constant temperature (with a thermostat),

ensuring consecutive introduction of the initial solutions and continuous mechanical stirring of the reaction mixture with a magnetic stirrer. The experiments were run at room temperature and atmospheric pressure. The reduction process was completed in 2 minutes, adding the reducing agent dropwise. Fine powder precipitates were obtained. They were filtrated, washed with distillate water and alcohol, and dried in a vacuum oven for 24 hours at 100°C.

Co-Sn nanoparticles (Co:Sn = 35:65) were also synthesized applying a template technique using a carbon-containing support of fluorinated graphite (CF) and graphite, in the presence of β -cyclodextrine (β -CDx). Thus, the carbon-based nanocomposites were obtained in situ. The technological conditions (concentration and quantity of the initial reaction solutions, reducing agent and ligand) were the same.

The quantity of the fluorinated graphite CF, used as a support was 0.247 g. The ratio of support to nanoparticles was 20 % : 80 %. When using fluorinated graphite in the presence of β -cyclodextrine, we used equal quantities of CF and β -CDx – 0.306 g. In this case the ratio CF/ β -CDx/Co-Sn nanoparticles has been 20 % CF : 20 % β -CDx : 60 % Co-Sn nanoparticles.

Synthesis of intermetallic Ni-Sn nanoparticles at a ratio Ni:Sn = 45:55 and their carbon-containing nanocomposites

Synthesis of intermetallic Ni-Sn nanoparticles was carried out through the borohydride reduction method with 0.2M NaBH₄ in a mixture of aqueous solutions of 0.1M NiCl₂·6H₂O and 0.1M SnCl₂·2H₂O, at a mass ratio Ni:Sn=45:55, in accordance with the phase diagram of the binary Ni-Sn system, consecutively introducing the initial solutions of the chloride salts and the reducing agent. Citric acid C₆H₈O₇ was used, as a stabilizing agent, in a quantity of 0.4g/100 ml. The synthesis was accomplished in the same double-wall cell, described above, and at the same technological conditions - room temperature and atmospheric pressure.

A template synthesis of intermetallic Ni-Sn nanoparticles was also performed through the borohydride reduction with 0.2M NaBH₄ in a mixture of aqueous solutions of the corresponding chloride salts-hydrates (0.1M NiCl₂·6H₂O and 0.1M SnCl₂·2H₂O), at a ratio Ni:Sn=45:55. Fluorinated graphite (CF) was used as carbon-based support and β -cyclodextrine (β -CDx), as

a capping agent. In this manner, the carbon-based nanocomposites are obtained in situ. The quantity of the support was 20 % from the total volume of the synthesized nanoparticles, i.e. the mass ratio nanopartilces to graphite support was 80:20. After finishing the reduction process, the obtained precipitates were filtrated, washed with distillate water and alcohol, and dried in a vacuum oven at 100°C for 24 hours.

Investigating techniques

We used different techniques to characterize the synthesized intermetallic Co-Sn and Ni-Sn nanoparticles and their carbon-based nanocomposites. Their morphology, structure, elemental and phase composition were studied with Scanning electron microscopy (SEM), Transmission electron microscopy (TEM), Energy-dispersive X-ray spectroscopy (EDS) and X-ray diffraction analysis (XRD).

The SEM images were made with a JEOL 6390 (Japan) SEM microscope at accelerating voltage of 20 kV in three regimes: a secondary electron image (SEI regime), a back reflex electron composition image (BEC regime), and a split/shadow image, the so-called “combined regime (SPI regime)”. The SEI images give information for the investigated sample surface, while the BEC images – for its chemical composition. The dark regions of the BEC images characterize the existence of atoms with a lower atom number, while the light region brings information for existence of atoms with higher atom number. The TEM images were taken with Transmission electron microscope JEOL JEM-2100F, at accelerating voltage of 200 kV. The EDS analysis was made, using the same SEM microscope with a detector for Energy-dispersive X-ray spectroscopy. Additional EDS analysis was performed with an UHR-FEG-SEM (Zeiss Merlin) with SDD (Oxford Inst), at an accelerating voltage of 15 kV. The phase composition of the investigated samples was determined by X-ray diffraction (XRD). The X-ray diffraction patterns of all samples were collected within the 2 θ range from 10° to 95° with a constant step of 0.03° and a counting time of 1 s/step on a Philips PW 1050 diffractometer, using CuK α radiation. The electrochemical tests of the model electrode samples, based on the obtained nanocomposites with a carbon matrix and intermetallic (Co-Sn, Ni-Sn) nanoparticles as anodes, were done at room temperature by cycling voltammetry in a three-electrode cell (Li-ion battery),

using a laboratory cycle system BA502 Series Battery Analyzer with computer control [25 - 28]. The model electrode was the positive electrode (anode), prepared by spreading on one side the obtained C-matrix/nanoparticle composites of a Cu foil. The electrode composition was as follows: 80 % (w/o) anode materials, 10 mass % of TAB2 (Teflonized Acetylen Black), and 10 mass % of PVDF (polyvinylidenefluoride) binder in 1-methyl-2-pyrrolidinone (NMP) solvent to form a homogeneous slurry. The electrodes were dried at 120°C in a vacuum oven for 12 h and then pressed to enhance the contact between the active materials and the conductive carbons. Metallic Li foil was used as a counter electrode, while the reference electrode was Li/Li⁺. The electrolyte (dried) was 1M LiPF₆, dissolved in a mixture of ethylene carbonate (EC) and dimethylcarbonate (DMC) (1:1 in volume). The water content in the electrolyte was below 30 ppm. The test cell was assembled in a glove box, under argon. It was cycled at room temperature, respectively discharged and recharged at constant current densities with a 0.1 C rate between 50 and 1500 mV vs. Li/Li⁺. Cyclic voltammograms (CVs) were measured with a scan rate of 0.1mV/s, using a potentiostat in the same three electrode cells.

In the case of the anode composite material, based on graphite (CF) matrix and Co-Sn, respectively - Ni-Sn alloy, the composition of the active material was 80% intermetallic (Co-Sn, Ni-Sn) nanoparticles and 20% graphite (CF). In the case of a graphite matrix/ β -CDx, the composition was: 60 % Co-Sn, resp. Ni-Sn nanoparticles, 20 % graphite(CF) and 20 % β -CDx.

RESULTS AND DISCUSSION

Physicochemical characterisation of the obtained samples, based on co-ni nanoparticles, before conducting electrochemical tests

The SEM image, at a magnification x1000, of the

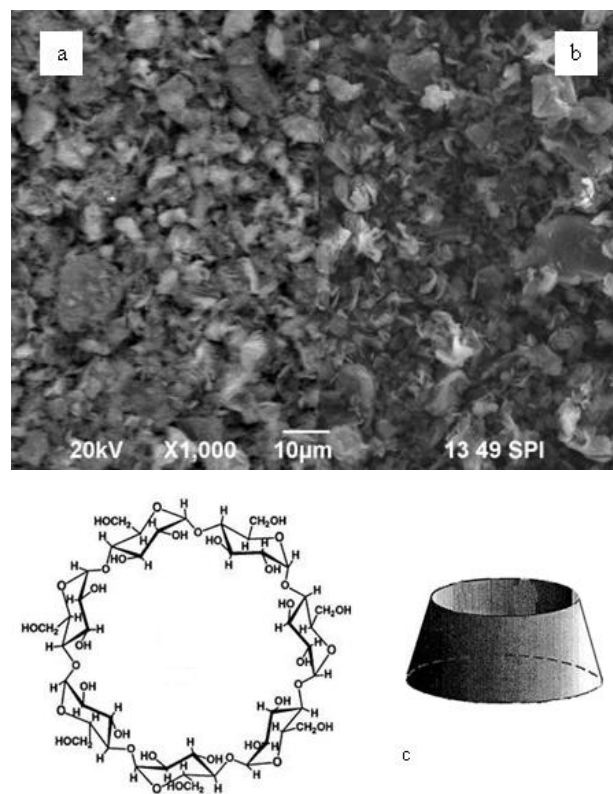


Fig. 1. SEM - SPI image of CF at magnification x1 000: a - BEC image, b - SEI image, c - graphic formula of the β -CDx.

fluorinated graphite (CF) used as a support for the template synthesis of Co-Sn nanoparticles (Co:Sn = 35:65) is shown on Fig. 1a, 1b, while Fig. 1c presents the graphic formula of the β -CDx used during the synthesis.

1. Investigation of the morphology and elemental composition of Co-Sn nanoparticles

Results from SEM/EDS analyses of Co-Sn nanoparticles, obtained at a ratio Co:Sn=35:65.

The SEM image of Co-Sn nanoparticles, synthesized at a ratio Co:Sn = 35:63 is presented in Fig. 2, while the EDS results are given in Fig. 3.

Table 1. Data for the elemental composition of the sample in sp4 point.

Element	App	Intensity	Weight %	Weight %	Atomic %
	Conc.	Corrn.		Sigma	
O K	0.24	0.3431	18.24	1.80	57.23
Cl K	0.07	1.0197	1.71	0.21	2.42
Co K	0.54	0.9489	15.11	0.74	12.87
Sn L	2.26	0.9208	64.94	1.57	27.47
Totals			100.00		

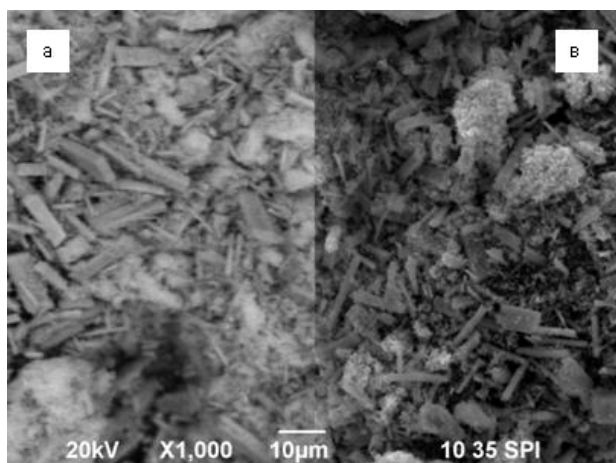


Fig. 2. SEM - SPI image of Co-Sn nanoparticles at a magnification $\times 1\,000$: a - BEC image, b - SEI image.

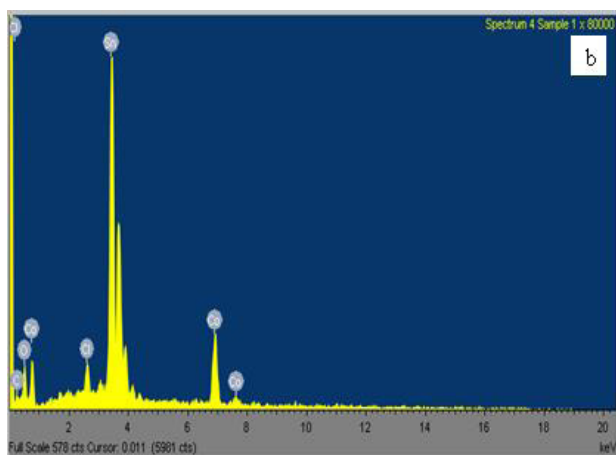
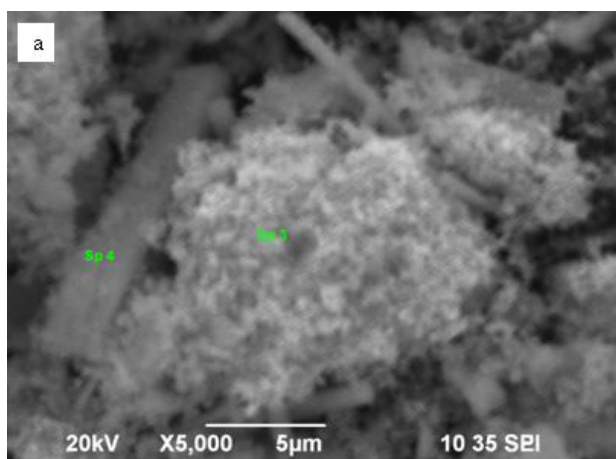


Fig. 3. Results from EDS analysis: a) SEM image at a magnification $\times 5\,000$ with indicated sp3 and sp4 points where EDS analysis is carried out, b) EDS spectrum for a distribution of the elements on the Co-Sn (Co:Sn = 35:65) nanoparticle surface in the sp4 shown on the SEM image left point (spectrum 4).

The SEM image of the Co-Sn nanoparticles, obtained at a ratio Co:Sn = 35:65 shows a morphology typical for alloyed materials. Spherical particles and also particles irregular in shape are observed. The parallelepipeds, like particles formed between the others, are probably from Sn.

In Fig. 3a is presented the SEM image of the same sample at a magnification $\times 5000$ (Co:Sn = 35:65), and the two points where the EDS analysis has been carried out, are indicated. The EDS spectrum for the distribution of the Co and Sn elements on the nanoparticle surface in the sp4 point is shown in Fig. 3b, while the elemental composition of the investigated sample in the same point, is given in Table 1.

Based on the results from the EDS analysis it could be concluded that the ratio Co:Sn = 35:65, set up in the initial solutions, was approximately preserved in the synthesized Co-Sn nanoparticles.

Results from TEM/EDS analyses of Co-Sn nanoparticles, obtained at a ratio Co:Sn = 3:2

The TEM images of the Co-Sn nanoparticles, synthesized at a ratio Co:Sn = 3:2 are presented in Fig. 4.

The Co-Sn nanoparticles, synthesized at a ratio Co:Sn = 3:2, are spherical in shape and their size is 50

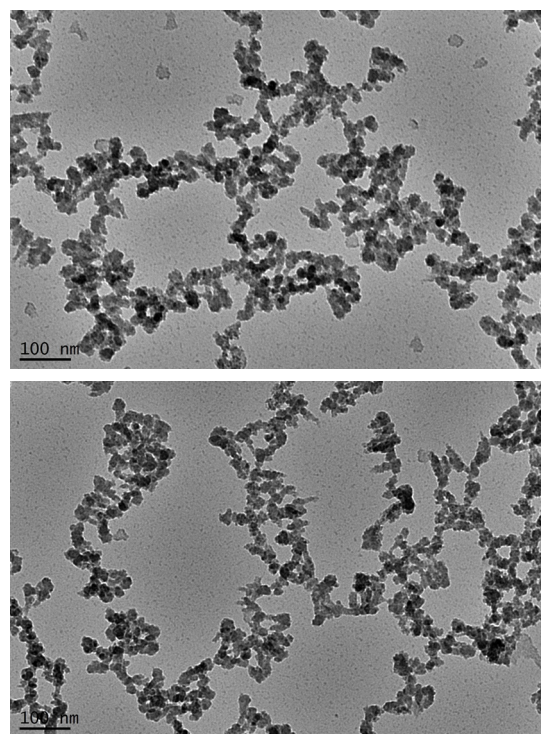


Fig. 4. TEM images of Co-Sn nanoparticles (Co:Sn = 3:2).

- 70 nm. Even though they formed spontaneous aggregates, the particles are monodisperse. The TEM images show good size distribution, that is favorable for their application as electrodes in Li-ion batteries.

The SEM image of the Co-Sn (Co:Sn = 3:2) nanoparticle surface, where the EDS analysis has been performed, is shown in Fig. 5a. The analysis was done with

an EDS detector in order to investigate the distribution of the elements on the surface and in the volume of the obtained nanoparticles (the so-called “mapping”). Fig. 5b presents a layered EDS image of all elements contained in the sample, while in Fig. 5c their distribution is given. Fig. 5d is the EDS spectrum. It can be clearly seen, that both the Co and the Sn elements are uniformly

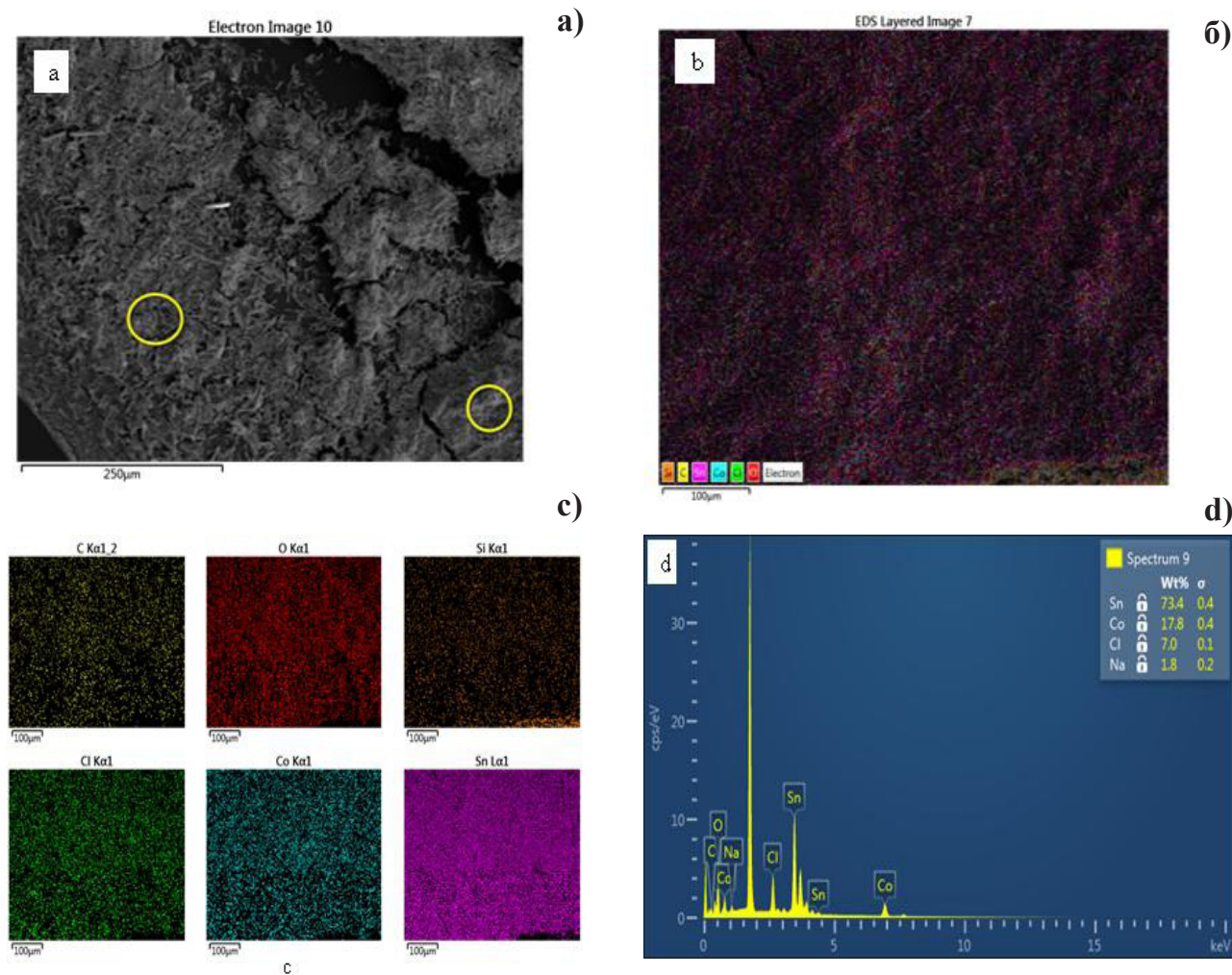


Fig. 5. Results from EDS analysis for Co-Sn nanoparticles (Co:Sn = 3:2): a-SEM image on the surface, b – layered image, c- EDS spectrum of the element distribution on the nanoparticle surface.

Table 2. Data for the elemental composition of the sample in sp8 point.

Element	App	Intensity	Weight %	Weight %	Atomic %
	Conc.	Corrn.		Sigma	
O K	0.73	0.3938	35.35	1.46	77.11
F K	0.00	0.6514	0.00	0.00	0.00
Cl K	0.09	1.0048	1.77	0.18	1.74
Co K	0.42	0.9061	8.93	0.52	5.29
Sn L	2.50	0.8877	53.95	1.30	15.86
Totals			100.00		

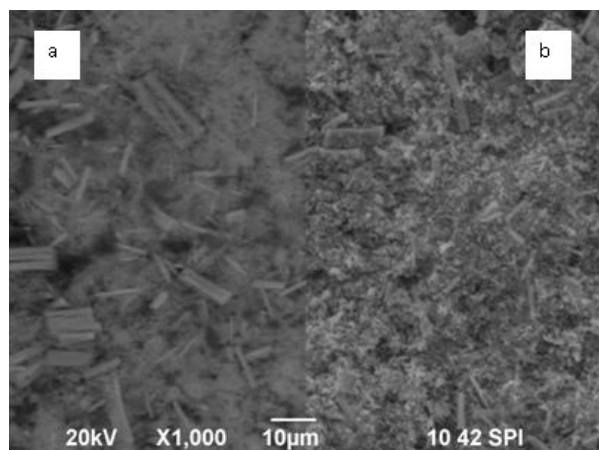


Fig. 6. SEM-SPI image of Co-Sn/CF nanocomposites at a magnification x1 000: a- BEC image, b- SEI image.

distributed, providing another confirmation that the synthesis of crystal intermetallic Co-Sn nanoparticles is successful. On some places the color representing Sn is more saturated, which is also in line with the observed formation of rod-shape Sn particles.

Investigation of the morphology and elemental composition of nanocomposites based on Co-Sn (Co:Sn = 35:65) nanoparticles and fluorinated graphite (CF). Results from SEM/EDS analyses

The SEM image at a magnification x1000 of the nanocomposites based on Co-Sn (Co:Sn = 35:65) nanoparticles and a fluorinated graphite matrix, is given in Fig. 6. The graphite used as a support is characterized by a flake-like structure (Fig. 1) that has influenced the formation of the intermetallic nanoparticles during their synthesis. The particle morphology is similar to that of the graphite: particles irregular in shape, such as the flake-like particles of the graphite, can be seen. Rod-shape particles, probably from Sn, can also be observed. The morphology is typical for alloyed materials. The particles exhibit a tendency to aggregate, which is a characteristic of the nanostate.

A SEM image of Co-Sn nanoparticles (Co:Sn = 35:65)/graphite (CF) composites, at magnification x5000, is presented in Fig. 7a. The two points where the EDS analysis is carried out are indicated. The EDS spectrum for the distribution of the Co and Sn elements on the nanoparticle surface in the sp⁴ point is shown in Fig. 7-b, while the elemental composition (at.% and mass %) of the investigated sample in the same point, is given in Table 2.

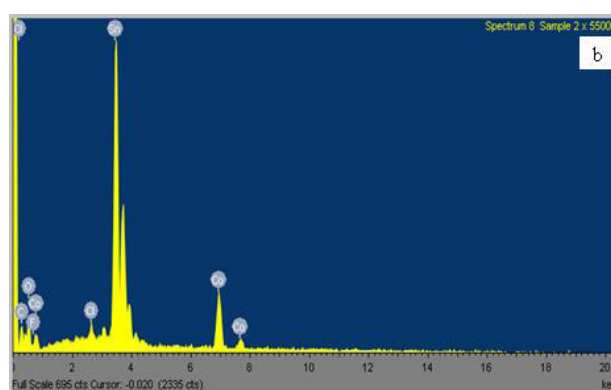
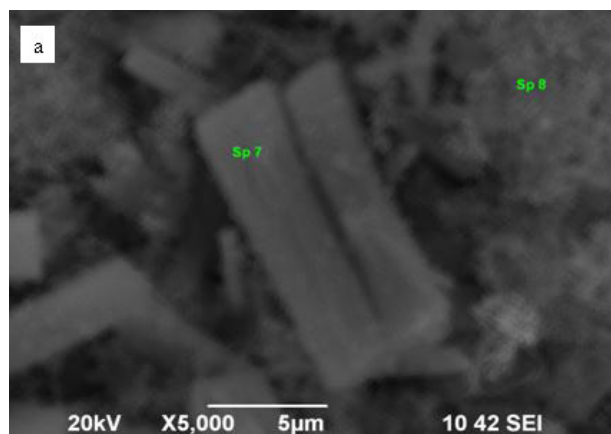


Fig. 7. Results from the EDS analysis: a- SEM image at magnification x5 000 with indicated sp7 and sp8 points where EDS analysis is carried out, b-EDS spectrum for a distribution of the elements on the surface of the Co-Sn/CF nanocomposite in sp8 point.

Investigation of the morphology and elemental composition of nanocomposites based on Co-Sn (Co:Sn = 35:65) nanoparticles, fluorinated graphite (CF) and β -cyclodextrine (β -CDx). Results from SEM/EDS analyses.

The structure of the β -cyclodextrine (β -CDx), used in the synthesis, is a hollow sphere, with functional groups situated on its surface (Fig. 2). It has to cover the synthesized nanoparticles and to prevent their aggregation.

The SEM image at magnification x1000 of nanocomposites based on Co-Sn (Co:Sn = 35:65), CF and β -CDx, is given in Fig. 8.

Fig. 9a is a SEM image of Co-Sn nanoparticles (Co:Sn = 35:65)/CF/ β -CDx composites, at magnification x5000. Again two points of sp¹¹ and sp¹², where EDS

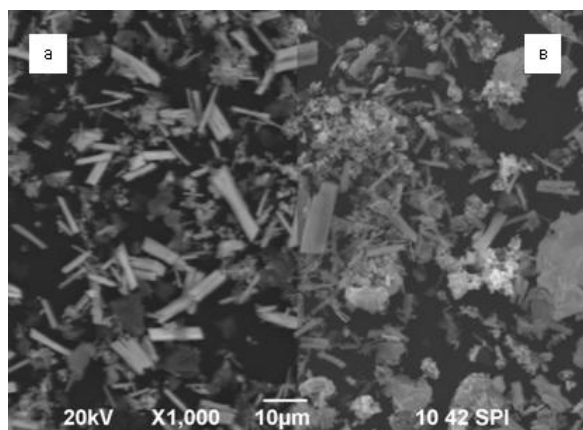


Fig. 8. SEM-SPI image of Co-Sn/CF/β-CDx Composite at a magnification x1 000: a- BEC image, b-SEI image.

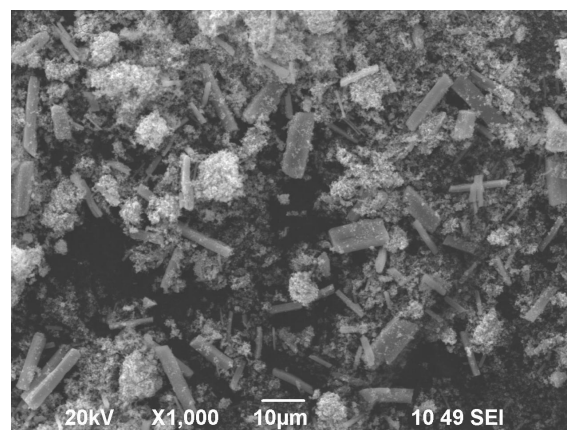


Fig. 10. SEM-SEI image of Ni-Sn nanoparticles at a magnification x1 000.

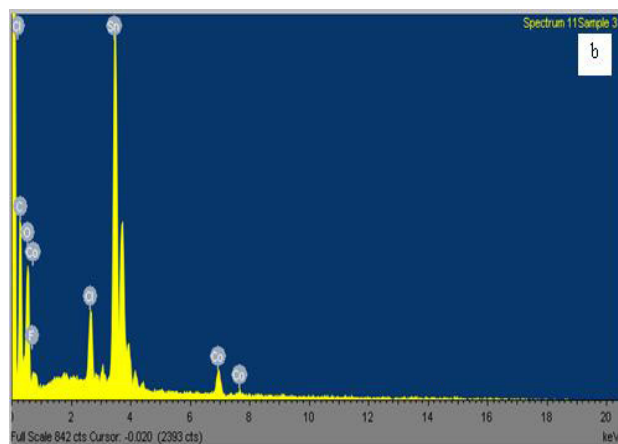
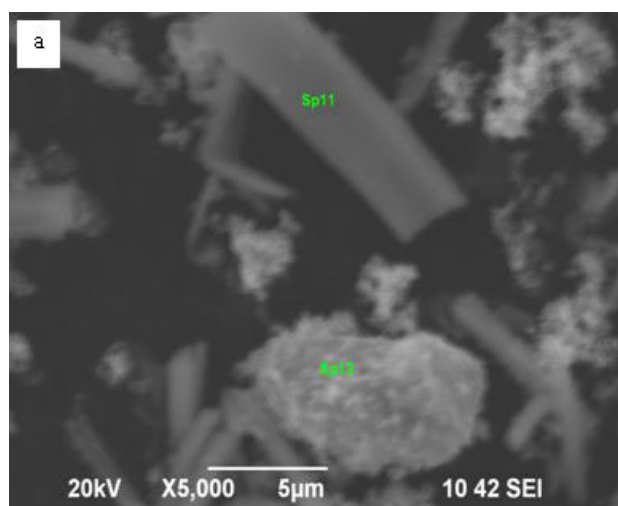


Fig. 9. Data from EDS analysis of Co-Sn alloy/CF/β-CDx composite: a-SEM image at a magnification x5 000 with indicated two points of sp11 and sp12 where EDS analysis is carried out, b-EDS spectrum for a distribution of the elements on the surface of the Co-Sn/CF/β-CDx nanocomposite in sp11 point.

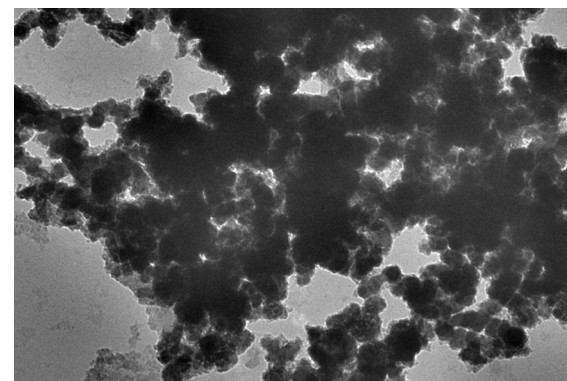
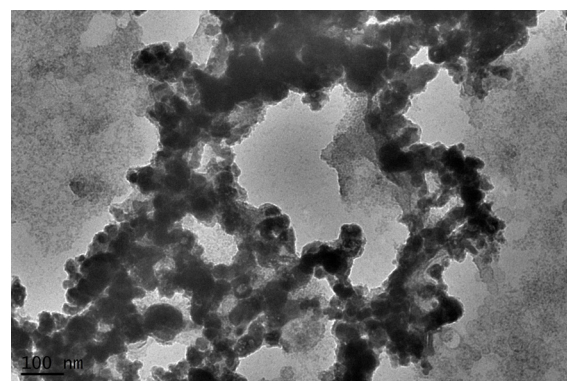
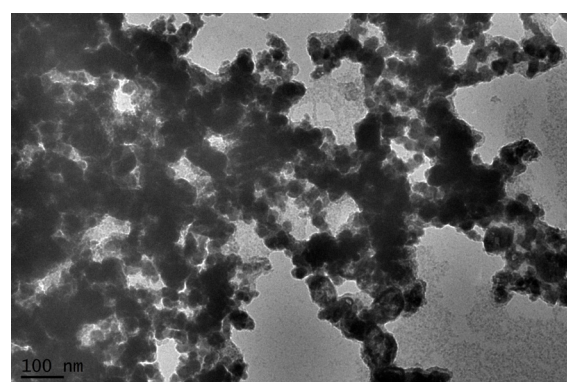


Fig. 11. TEM images of Ni-Sn nanoparticles (Ni:Sn = 3:2).

Table 3. Data for the elemental composition of the sample in sp11 point.

Element	App	Intensity	Weight%	Weight%	Atomic%
	Conc.	Corrn.		Sigma	
O K	1.19	0.4097	38.20	1.30	74.96
F K	0.20	0.6388	4.10	0.93	6.77
Cl K	0.23	1.0038	2.99	0.17	2.65
Co K	0.29	0.8911	4.28	0.34	2.28
Sn L	3.36	0.8738	50.44	1.19	13.34
Totals			100.00		

analysis is carried out, are indicated. The EDS spectrum for the distribution of the Co and Sn elements on the sample surface in the sp¹¹ point, is shown in Fig. 9-b, while the elemental composition (at.% and mass %) of the investigated sample in the same point is given in Table 3.

Investigation of the morphology and elemental composition of Ni-Sn nanoparticles. Results from the SEM/EDS analyses of Ni-Sn nanoparticles, obtained at ratio Ni:Sn = 45:55

The SEM image of the Ni-Sn nanoparticles, synthesized through borohydride reduction with NaBH₄, at a

ratio Ni:Sn=45:55, are presented in Fig. 10. The image is made at a magnification of x1000. It shows that the Ni-Sn nanoparticles have different sizes. Smaller particles of 20-30 nm and also bigger particles, irregular in shape that probably are from Sn, are observed.

Results from TEM/EDS analyses of Ni-Sn nanoparticles obtained at a ratio Ni:Sn = 3:2

TEM images of Ni-Sn nanoparticles, obtained at a ratio Ni:Sn = 3:2, are shown in Fig. 11, while the results from EDS analysis are given in Fig. 12 (a-d).

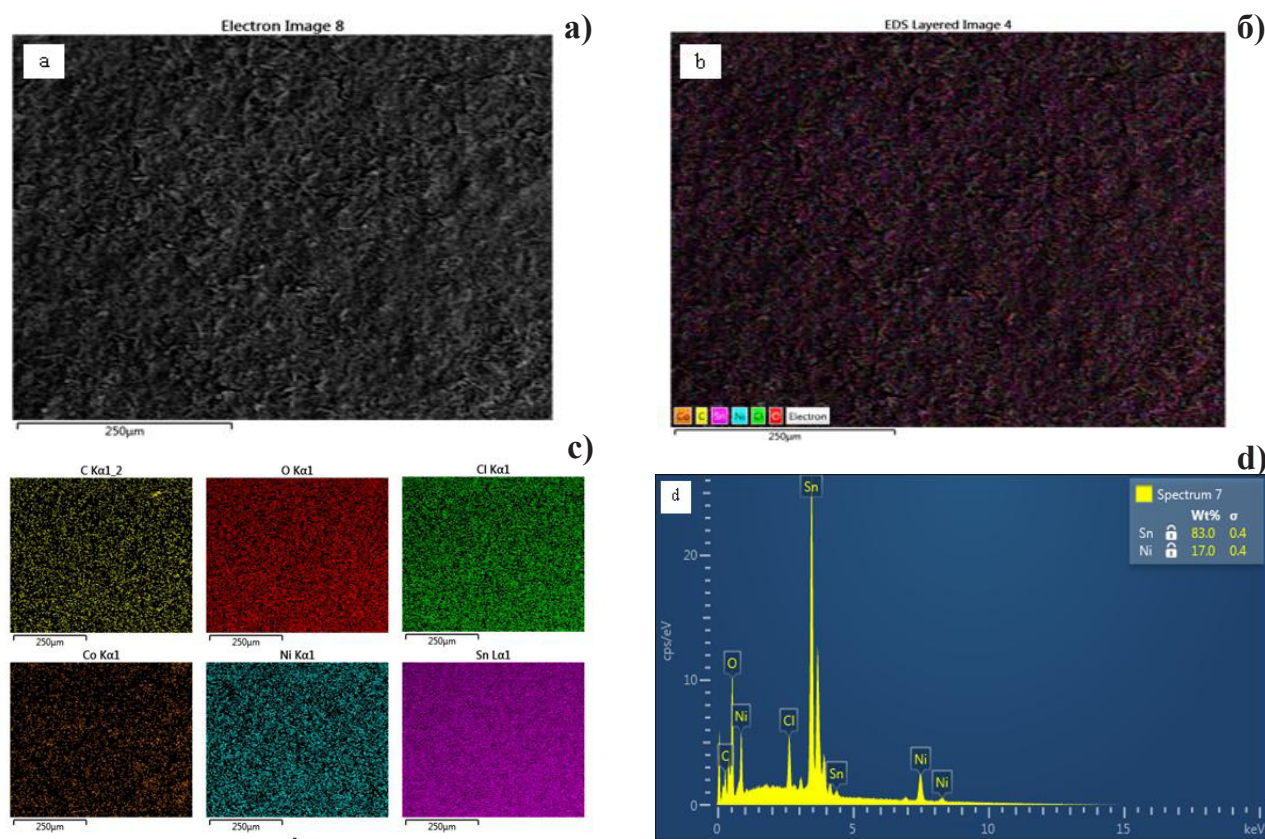


Fig. 12. Results from EDS analysis for Ni-Sn nanoparticles (Ni:Sn=3:2): a - SEM image of the surface, b - layered image, c - EDS spectrum of the element distribution on the nanoparticle surface.

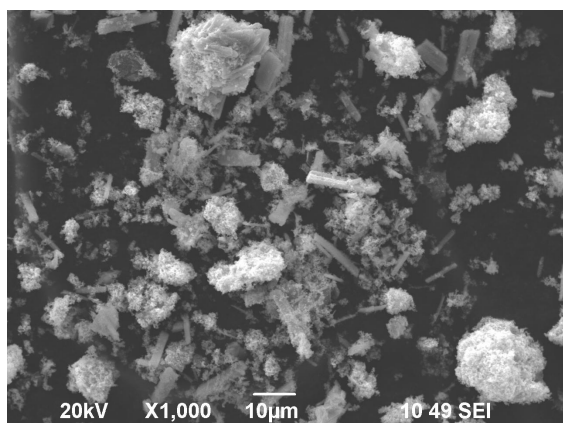


Fig. 13. SEM-SEI image of Ni-Sn/CF nanocomposites at a magnification x1 000.

Investigation of the morphology and elemental composition of nanocomposites, based on Ni-Sn (Co:Sn = 45:55) nanoparticles and fluorinated graphite (CF). Results from SEM/EDS analyses

SEM image at a magnification of x1000 of a carbon-containing nanocomposite, based on Ni-Sn (Ni:Sn = 45:55) nanoparticles and a fluorinated graphite matrix, is given in Fig. 13. The ratio of Ni-Sn alloy to the graphite support is 80 % : 20 %.

When fluorinated graphite is used as support, the SEM image shows flake-shape particles. This morphology is typical for the morphology of the graphite itself. The synthesized intermetallic nanoparticles are of the type Ni-Sn core/carbon shell.

In Fig. 14 are given the results from the EDS analysis, for the distribution of Ni and Sn elements on the surface of Ni-Sn (Ni:Sn = 45:55)/nanoparticles/graphite matrix composite, made in the sp¹⁷ point, shown on the SEM image (Fig. 14a). The elemental composition (at. % and mass %), taken in the same point on the surface of the investigated sample, is presented in Table 4.

On the basis of the results, obtained from the EDS analysis it can be concluded that the ratio Ni:Sn = 45:55 set up in the initial solutions is also preserved in the synthesized Ni-Sn nanoparticles, when a graphite is used as the support. Investigation of the phase composition of Co-Sn nanoparticles, obtained at ratio Co:Sn=35:65 and Ni-Sn, obtained at ratio Ni:Sn = 45:55, and of carbon-containing composites, based on them. The XRD patterns of Co-Sn nanoparticles, obtained at ratio Co:Sn=35:65 and Ni-Sn, at ratio Ni:Sn = 45:55, as well as of carbon-containing composites on their basis, are given in Figs. 15 and 16.

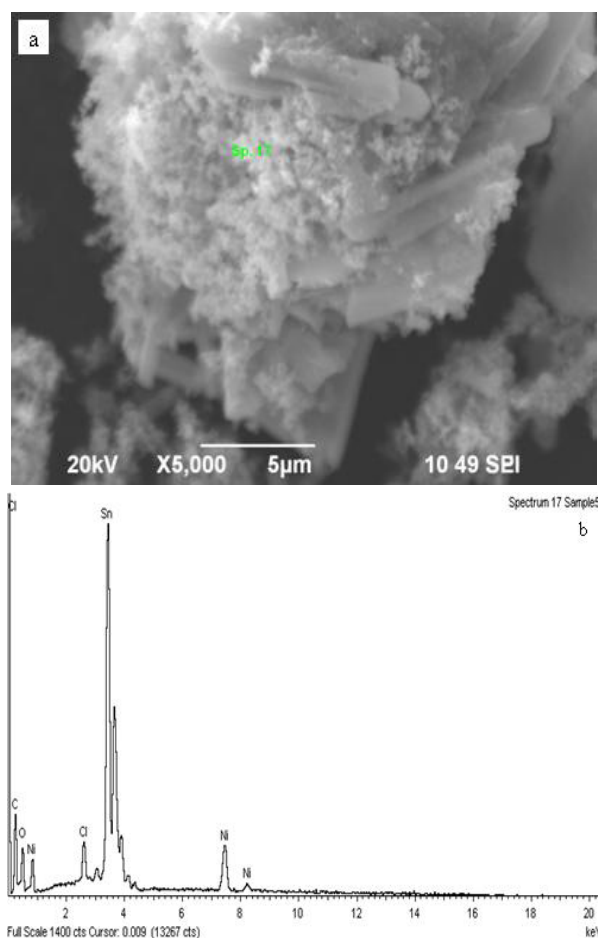


Fig. 14. Results from EDS analysis of a Ni-Sn nanoparticles/graphite composite: a-SEM image with an indicated sp¹⁷ pint, b-EDS spectrum for a distribution of the elements in sp¹⁷ pint.

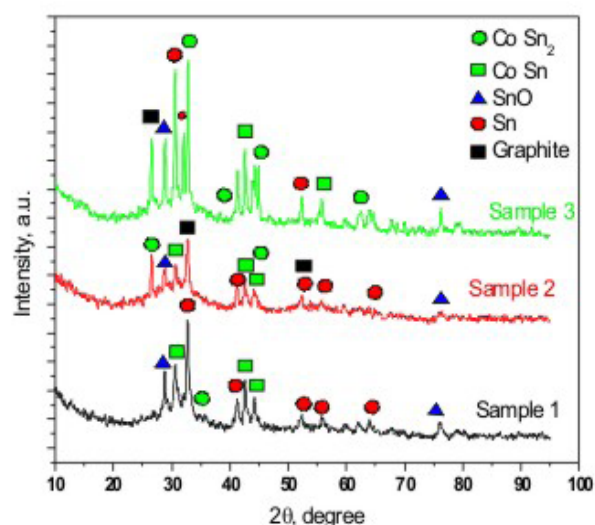


Fig. 15. XRD patterns: sample 1–Co-Sn particles (Co:Sn = 35:65); sample 2–Co-Sn particles/CF composite; sample 3– Co-Sn particles/CF/β-CDx composite.

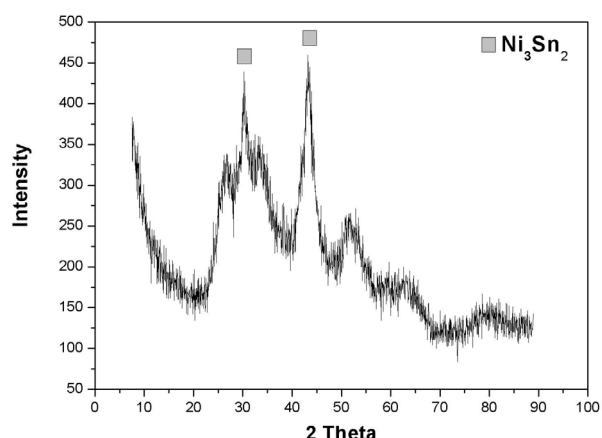


Fig. 16. XRD pattern of Ni-Sn nanoparticles synthesized at a ratio Ni:Sn = 45:55.

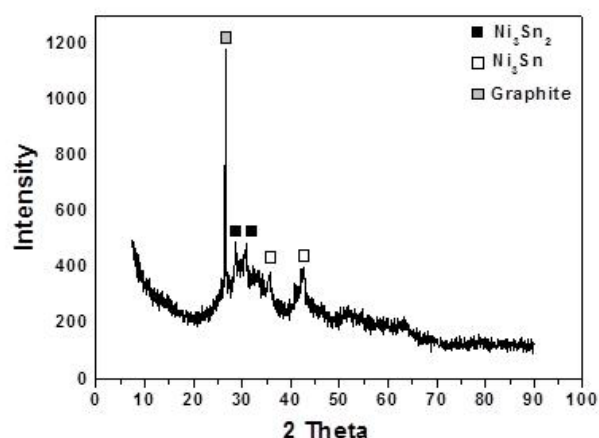


Fig. 17. XRD pattern of CF/Ni-Sn (Ni:Sn = 45:55) nanoparticles composite.

The XRD spectra of Co-Sn nanoparticles and their carbon-containing composites, show that in the synthesis of Co-Sn (Co:Sn = 35:65) nanoparticles, and also when using a carbon-based support, two main phases of CoSn_2 and CoSn , in accordance with the phase diagram of the binary Co-Sn system, are formed. A phase of Sn is also observed, as already known from the SEM images. A phase of graphite is detected, as well. The impurity of SnO phase is due to oxidizing processes.

The XRD pattern of a carbon-based nanocomposite with Ni-Sn nanoparticles, synthesized at ratio Ni:Sn = 45:55, with graphite as a carbon support, is presented in Fig. 17.

In the case of Ni-Sn nanoparticles, synthesized at a Ni:Sn = 45:55 ratio, the XRD analysis proves the formation of a Ni_3Sn_2 phase, while in the case of carbon-based nanocomposites with Ni-Sn nanoparticles (Ni:Sn = 45:55) and graphite matrix CF, two main phases of

Ni_3Sn_4 and Ni_3Sn are formed. According to literature data, the Ni_3Sn_4 phase exhibits better properties in electrochemical tests as an electrode material in Li-ion battery. This means that the graphite (CF) is a more appropriate matrix for obtaining composites on the base of Ni-Sn alloy for electrode materials.

STUDY OF THE MORPHOLOGY AND ELEMENTAL COMPOSITION OF THE OBTAINED SAMPLES, AFTER RUNNING ELECTROCHEMICAL TESTS

Study of the morphology of a nanocomposite, based on Co-Sn nanoparticles (Co:Sn = 35:65) and graphite matrix, after running electrochemical tests

Figs. 18 and 19 show SEM images of a CF matrix/Co-Sn particles nanocomposite, after the electrochemical tests are run. Images at different magnification, in

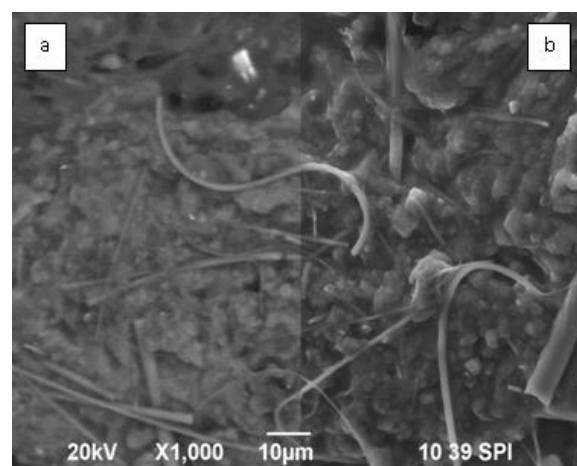


Fig. 18. SEM-SPI image of Co-Sn/CF nanocomposites at a magnification x1 000: a- BEC image, b- SEI image.

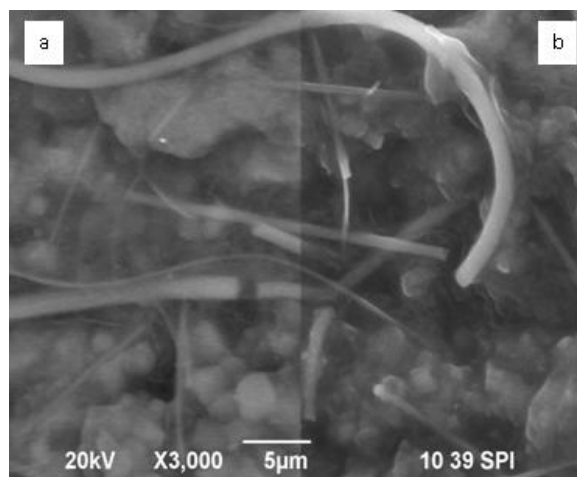


Fig. 19. SEM-SPI image of Co-Sn/CF nanocomposites at a magnification x3 000: a- BEC image, b- SEI image.

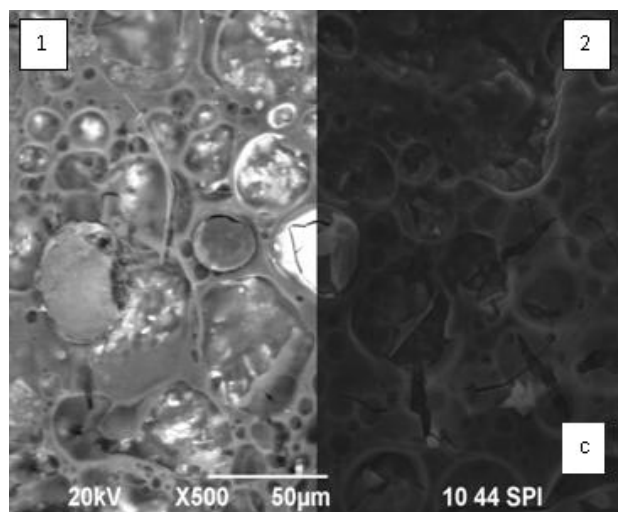
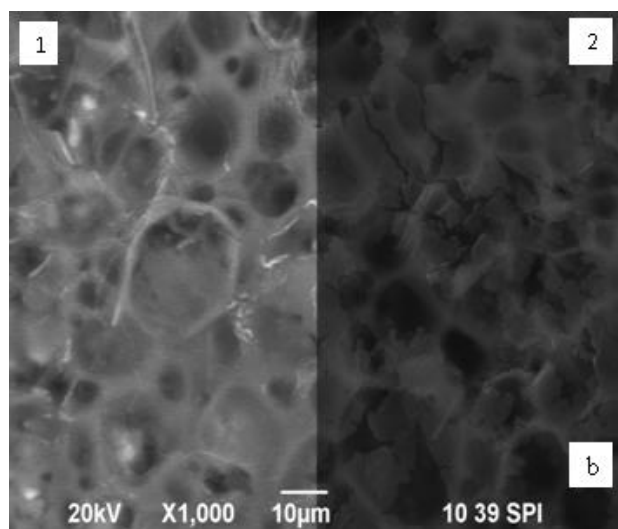
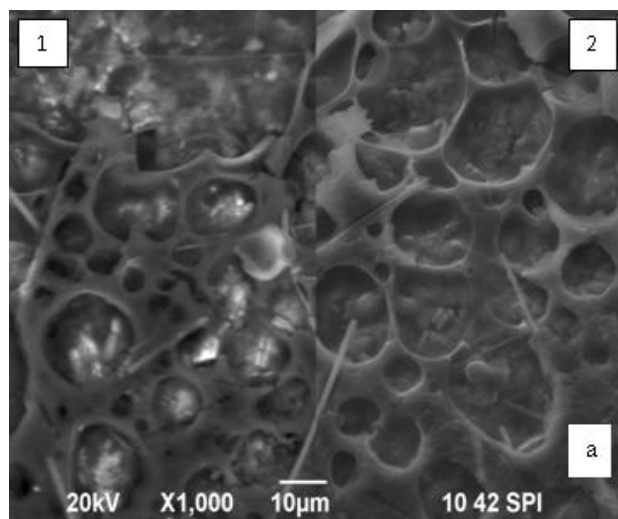


Fig. 20. SEM-SPI image of Co-Sn/CF/β-CDx composite at magnification: a, b -x1000, c-x500; 1- BEC image, 2 – SEI image.

a mixed imaging mode – back scattered electrons and secondary electrons, are presented.

The images show that the electrodes, based on a CF matrix and a Co-Sn alloy (Co:Sn = 35:65), remain dense and homogeneous. No visible cracking is observed after the electrochemical tests are run.

Study of the morphology of a nanocomposite, based on Co-Sn nanoparticles (Co:Sn = 35:65), a graphite matrix and β-cyclodextrine (β-CDx), after running the electrochemical tests

Fig. 20 shows SEM images of a CF matrix/Co-Sn particles and a β-cyclodextrine nanocomposite, after the electrochemical tests are performed. Presented are images at a different magnification in a mixed imaging mode – back-scattered electrons and secondary electrons. The SEM images show that the electrode material, based on Co-Sn nanoparticles, a CF matrix, and β-CDx remains like an unbroken network. The material's porous

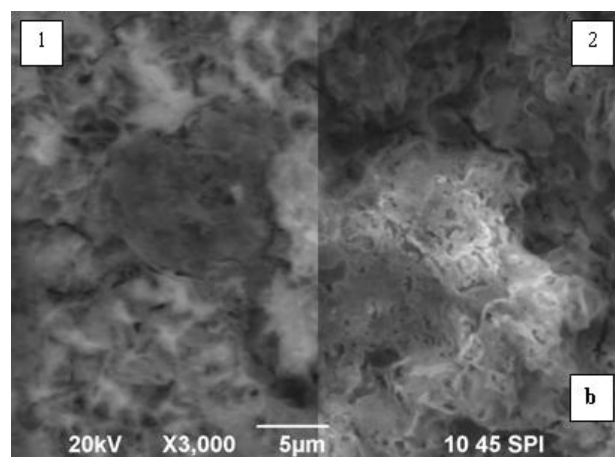
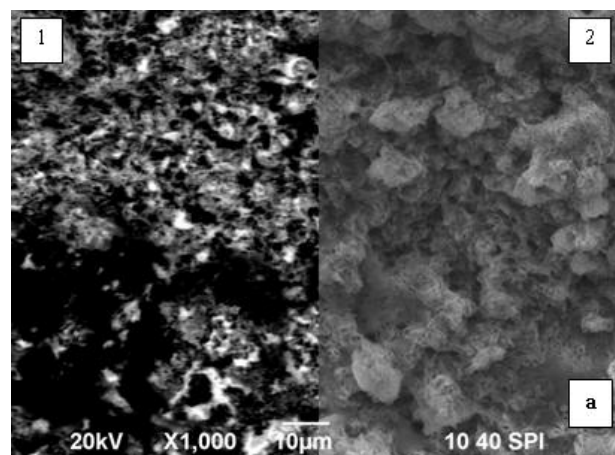


Fig. 21. SEM-SPI image of Ni-Sn/CF composite at a magnification: a-x1000, b-x3000; 1- BEC image, 2 – SEI image.

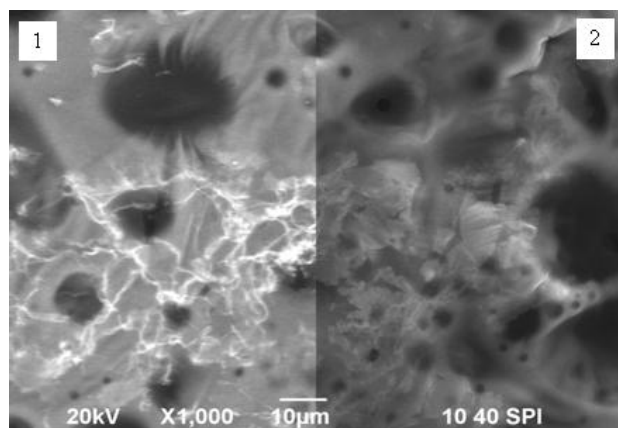


Fig. 22. SEM-SPI image of Ni-Sn/CF/β-CDx composite at magnification x1000; 1- BEC image, 2 – SEI image.

structure buffers the volume change during lithiation/delithiation processes.

Study of the morphology of a nanocomposite, based on Co-Sn nanoparticles (Co:Sn = 45:55), and a graphite matrix (ratio nanoparticles:graphite = 80 %:20 %), after running the electrochemical tests.

Fig. 21 shows SEM images of a CF matrix/Ni-Sn particles nanocomposite, after electrochemical tests are performed. The presented images are at different magnification in a mixed imaging mode – back-scattered electrons (BEC) and secondary electrons (SEI).

Study of the morphology of a nanocomposite, based on Ni-Sn nanoparticles (Co:Sn=45:55), a graphite matrix and β-cyclodextrine (β-CDx), after running the electrochemical tests

Fig. 22 shows the SEM images of a CF matrix/Ni-Sn particles and a β-CDx nanocomposite, after the electrochemical tests are performed. Presented are images at a magnification x1000 in a mixed imaging mode – back-scattered electrons and secondary electrons. Combining a carbon matrix and intermetallic nanoparticles helps

reducing the mechanical stress, caused by the lithiation/delithiation processes, during the charge/discharge cycles. This prolongs and improves the cycling life of the battery. The electrochemical tests of the nanocomposites, based on a Co-Sn, Ni-Sn alloy and a CF matrix, show that these composites have significantly higher capacity, as compared to the capacity of pure alloys [27, 28].

CONCLUSIONS

The template synthesis through a borohydrate reduction, using carbon (graphite CF and β-cyclodextrine), proves to be an effective way to obtain in situ new carbon based composites with active intermetallic Co-Ni and Ni-Sn nanoparticles, for electrodes in batteries. The fine Co-Sn and Ni-Sn powder prepared has a morphology, typical for alloys and can successfully replace graphite as an anode material in Li-ion batteries.

The CF matrix is suitable in terms of obtaining fine mono dispersed nanoparticles with wide size distribution. The particles are 40 to 80 nm in size. They have irregular shape and tend to aggregate spontaneously. Aggregates, ranging from 200 to 300 nm are observed. To avoid that, β-cyclodextrine has been used as a capping agent.

The X-ray diffraction analysis of the Co-Sn and Ni-Sn particles and their carbon based composites, with a matrix of graphite, proved that at a mass ratio of Co:Sn = 35:65, set in the synthesis of the particles, two main phases of CoSn₂ and CoSn were formed, while the Ni-Sn particles and their carbon based composites, using a graphite matrix at a mass ratio Ni: Sn = 45:55, formed three main phases of Ni₃Sn₂, Ni₃Sn₄ and Ni₃Sn. This is in accordance with the phase diagrams of the Co-Sn and Ni-Sn binary systems.

The SEM studies of the model electrodes, based on

Table 4. Data for the elemental composition of Ni-Sn alloy/graphite composite.

Element	Intensity	mass %	mass %	atomic %
O K	0.8128	15.87	0.70	43.28
	0.3393	16.29	0.94	33.34
Cl K	0.8674	2.00	0.13	1.85
Ni K	0.9504	11.93	0.44	6.65
Sn L	0.8814	53.91	0.84	14.88
Totals		100.00		

the synthesized intermetallic nanoparticles with a graphite matrix and the use of β -cyclodextrin, conducted after running electrochemical tests, show that the morphology, the nanostructure and the crystallinity of the samples have not changed. After the electrochemical testing, the samples remain homogeneous and dense, with no signs of cracking. They are not destroyed during the processes of charge and discharge. The SEM images show that after electrochemical testing, the model electrodes, based on intermetallic Co-Sn and Ni-Sn nanoparticles, respectively, retain their mechanical integrity and strength. This can be explained by the presence of the inactive component (Ni and Co), which acts as a buffer.

Co-Ni and Ni-Sn particles, synthesized using a graphite matrix, kept their flake shape, after the electrochemical tests are performed. This shape is similar to the shape of the substrate (graphite) and is identical to the shape of the particles, before carrying out the electrochemical tests. In case of using graphite, in the presence of β -cyclodextrin, the SEM images reveal that the lattice of β -cyclodextrin has not changed and its entirety is retained during the electrochemical tests. We assume that this lattice buffers the volume expansion, which occurs in the lithiation/delithiation processes during the charge/discharge cycles.

Acknowledgements

Special thanks to Assoc. Prof. Dr Toma Stankulov from IEES at the Bulgarian Academy of Sciences for the electrochemical tests taken of the investigated samples.

REFERENCES

1. H. Groult, H. El Ghallali, A. Barhoun, E. Briota, C.M. Julien, F. Lantelmea, S. Borensztjand, Study of Co-Sn and Ni-Sn alloys prepared in molten chlorides and used as negative electrode in rechargeable lithium battery, *Electrochimica Acta*, 56, 2011, 2656-2664.
2. Xiao-Yong Fan, Fu-Sheng Ke, Guo-ZhenWei, Ling Huang, Shi-Gang Sun, Sn-Co alloy anode using porous Cu as current collector for lithium ion battery, *J. Alloys and Compounds*, 476, 2009, 70-73.
3. M. Valvo, U. Lafont, L. Simonin, E.M. Kelder, Sn-Co compound for Li-ion battery made via advanced electrospraying, *J. Power Sources*, 174, 2007, 428-434.
4. Ling Huang, Hong-BingWei, Fu-Sheng Kea, Xiao-Yong Fan, Jun-Tao Li, Shi-Gang Sun, Electrodeposition and lithium storage performance of three-dimensional porous reticular Sn-Ni alloy electrodes, *Electrochimica Acta*, 54, 2009, 2693-2698.
5. Chunhui Tan, Gongwei Qi, Yeping Li, Jing Guo, Xin Wang, Delong Kong, Hongjun Wang, Shuyong Zhang, Performance enhancement of Sn-Co alloys for lithium-ion battery by electrochemical dissolution treatment, *J. Alloys and Compounds*, 574, 2013, 206-211.
6. Bo-Ok Jang, Seok-Hwan Park, Wan-Jin Lee, Electrospun Co-Sn alloy/carbon nanofibres composite anode for lithium ion batteries, *J. Alloys and Compounds*, 574, 2013, 325-330.
7. Jianchao He, Hailei Zhao, Jing Wang, Jie Wang, Jingbo Chen, Hydrothermal synthesis and electrochemical properties of nano-sized Co-Sn alloy anodes for lithium ion batteries, *J. Alloys and Compounds*, 508, 2010, 629-635.
8. Jianchao He, Hailei Zhao, Mengwei Wang, Xidi Jia, Preparation and characterization of Co-Sn-C anodes for lithium-ion batteries, *Materials Science and EngineeringB*, 171, 2010, 35-39.
9. Cheng Yang, Dawei Zhang, Yongbin Zhao, Yuhao Lu, Long Wang, John. B. Goodenough, Nickel foam supported Sn-Co alloy film as anode for lithium ion batteries, *J. Power Sources*, 196, 2011, 10673-10678.
10. Wang Zhang, Ming Chen, Xiangdong Gong, Guowang Diao, Universal water-soluble cyclodextrin polymer-carbon nanomaterials with supramolecular recognition, *Carbon*, 6, I, 2013, 154-163.
11. Hong Guo, Hailei Zhao, Xidi Jia, Xue Li, Weihua Qiu, A novel micro-spherical CoSn₃/Sn alloy composite as high capacity anode materials for Li-ion rechargeable batteries, *Electrochimica Acta*, 52, 2007, 4853-4857.
12. Ling Huang, Jin-Shu Cai, Yang He, Fu-Sheng Ke, Shi-Gang Sun, Structure and electrochemical performance of nanostructured Sn-Co alloy/carbon nanotube composites as anodes for lithium ion batteries, *Electrochemistry Communications*, 11, 2009, 950-953.
13. Heon-Yong Lee, Serk-Won Jang, Sung-Man Lee, Seung-Joo Lee, Hong-Koo Baik, Lithium Storage properties of nanocrystalline Ni₃Sn₄ alloys prepared by mechanical alloying, *J. power Sources*, 112, 2002, 8-12.
14. Z.P. Guo, Z.W. Zhao, H.K. Liu, S.X. Dou, Electrochemical lithiation and de-lithiation of MWNT-Sn/SnNi nanocomposites, *Carbon*, 43, 2005, 1392-1399.

15. H. Mukaibo, T. Osaka, T. Momma, Changes of electro-deposited Sn–Ni alloy thin film for lithium ion battery anodes during charge discharge cycling, *J. Power Sources*, 146, 2005, 457-463.
16. R.W. Scott, O.M. Wilson, R.M. Crooks, Synthesis, characterization, and applications of dendrimer-encapsulated nanoparticles, *J. Phys. Chem B*, 109, 2005, 692-704.
17. Hong Guo, Hailei Zhao, Xidi Jia, Spherical Sn–Ni–C alloy anode material with submicro/micro complex particle structure for lithium secondary batteries, *Electrochemistry Communications*, 9, 2007, 2207-2211.
18. H. El Ghallali, H. Groult, A. Barhoun, K. Draoui, D. Krulic, F. Lantelme, Electrochemical synthesis of Ni–Sn alloys in molten LiCl–KCl, *Electrochimica Acta*, 54, 2009, 3152-3160.
19. Ling Huang, Hong-Bing Wei, Fu-Sheng Kea, Xiao-Yong Fan, Jun-Tao Li, Shi-Gang Sun, Electrodeposition and lithium storage performance of three-dimensional porous reticular Sn–Ni alloy electrodes, *Electrochimica Acta*, 54, 2009, 2693-2698.
20. Arther T. Gates, Elizabeth G. Nettleton, V. Sue Myers, and Richard M. Crooks, Synthesis and Characterization of NiSn Dendrimer-Encapsulated Nanoparticles, *Langmuir*, 2010, 12994-12999.
21. Z. Edfouf, F. Cuevas, M. Latroche, C. Georges, C. Jordy, T. Hezeque, G. Caillon, J. C. Jumas, M. T. Sougrati, Nanostructured Si/Sn–Ni/C composite as negative electrode for Li-ion batteries, *J. power sources*, 196, 2011, 4762-4768.
22. Ruguang Ma, Zhouguang Lu, Shiliu Yang, Liuji-ang Xi, Chundong Wang, H.E. Wang, C.Y. Chung, Facile synthesis and electrochemical characterization of $\text{Sn}_4\text{Ni}_3/\text{C}$ nanocomposites as anode materials for lithium ion batteries, *J. Solid State Chemistry*, 196, 2012, 536-542.
23. H. El Ghallali, H. Groult, A. Barhoun, K. Draoui, D. Krulic, F. Lantelme, Electrochemical synthesis of Ni–Sn alloys in molten LiCl–KCl, *Electrochimica Acta*, 54, 2009, 3152-3160.
24. You Kyeong Jeong, Tae-woo Kwon, Inhwa Lee, Taek-Soo Kim, Ali Coskun, Jang Wook Choi, Hyperbranched β -Cyclodextrin Polymer as an Effective Multidimensional Binder for Silicon Anodes in Lithium Rechargeable Batteries, *Nano Lett.*, 14, 2, 2014, 864-870.
25. V. Milanova, T. Petrov, O. Chauvet, I. Markova, Study of Carbon-based nanocomposites with inter-metallic (Co–Sn, Ni–Sn) nanoparticles, *Rev. Adv. Mater. Sci.*, 37, 2014, 42-47.
26. I. Markova, V. Milanova, T. Petrov, I. Denev, O. Chauvet, New Porous Nanocomposite Materials for Electrochemical Power Sources, *Key Engineering Materials*, 644, 4, 129-132.
27. V. Milanova, I. Markova, M. Piskin, T. Stankulov, T. Petrov, I. Denev, Synthesis and study of carbon-based nanocomposites with Co–Sn nanoparticles for electrode materials, *J. Chem. Technol. Mater.*, 50, 3, 2015, 288-298.
28. V.L. Milanova, M.B. Piskin, T.I. Petrov, T.E. Stankulov, I.D. Denev, I.N. Markova, Ni–Sn alloy carbon-containing nanocomposites as alternative anode materials to the graphite electrodes in Li-ion batteries, *Rev. Adv. Mater. Sci.*, 41, 2015, 52-60.